ARMY RESEARCH LABORATORY

A Comparison of the Deformation, Flow, and Failure of Two Tungsten Heavy Alloys in Ballistic Impacts

by Brian Schuster and Lee Magness

ARL-RP-112 December 2005

A reprint from the *Proceedings of the International Conference on Refractory and Hard Metals*, 28–30 October 2002, Institute of Materials, UK.

NOTICES

Disclaimers

Army Research Laboratory
Aberdeen Proving Ground, MD 21005-5066

ARL-RP-112 **December 2005**

A Comparison of the Deformation, Flow, and Failure of Two Tungsten Heavy Alloys in Ballistic Impacts

Brian Schuster and Lee Magness
Weapons and Materials Research Directorate, ARL

A reprint from the *Proceedings of the International Conference on Refractory and Hard Metals*, 28–30 October 2002, Institute of Materials, UK.

REPORT DOCUMENTATION PAGE

Form Approved
OMB No. 0704-0188

1. REPORT DATE (*DD-MM-YYYY*)	2. REPORT TYPE	3. DATES COVERED (From - To)
December 2005	Reprint	28–30 October 2002

4. TITLE AND SUBTITLE
A Comparison of the Deformation, Flow, and Failure of Two Tungsten Heavy Alloys in Ballistic Impacts

5a. CONTRACT NUMBER

5b. GRANT NUMBER

5c. PROGRAM ELEMENT NUMBER

6. AUTHOR(S)
Brian Schuster and Lee Magness

5d. PROJECT NUMBER
68T8G8

5e. TASK NUMBER

5f. WORK UNIT NUMBER

7. PERFORMING ORGANIZATION NAME(S) AND ADDRESS(ES)
U.S. Army Research Laboratory
ATTN: AMSRD-ARL-WM-TC
Aberdeen Proving Ground, MD 21005-5066

8. PERFORMING ORGANIZATION REPORT NUMBER
ARL-RP-112

9. SPONSORING/MONITORING AGENCY NAME(S) AND ADDRESS(ES)

10. SPONSOR/MONITOR'S ACRONYM(S)

11. SPONSOR/MONITOR'S REPORT NUMBER(S)

12. DISTRIBUTION/AVAILABILITY STATEMENT
Approved for public release; distribution is unlimited.

13. SUPPLEMENTARY NOTES
A reprint from the *Proceedings of the International Conference on Refractory and Hard Metals*, 28–30 October 2002, Institute of Materials, UK.

14. ABSTRACT
Ballistic tests were conducted with subscale long rod penetrators of two different processing conditions of the same tungsten heavy alloy. The liquid-phase sintered composite of 90% tungsten-9% nickel–1% cobalt (by weight) was tested in its low-strength, as-sintered and heat-treated condition, and in a high-strength, 50% cold-worked (by swaging) and aged condition. Consistent differences in the ballistic performance of the two lots of penetrators were observed, in depth of penetrations test in thick armor steel targets and in limit velocity determinations against finite thickness steel targets. Metallographic examinations were conducted on the residual penetrators recovered from sectioned steel targets. Using the tungsten particles in the nickel alloy matrices of these residual penetrator materials as embedded strain gauges, the strain distributions, deformation gradients, and flow and failure behaviors of these two tungsten heavy alloy lots are examined.

15. SUBJECT TERMS
penetration, tungsten heavy alloy, deformation, failure

16. SECURITY CLASSIFICATION OF: a. REPORT	b. ABSTRACT	c. THIS PAGE	17. LIMITATION OF ABSTRACT	18. NUMBER OF PAGES	19a. NAME OF RESPONSIBLE PERSON
UNCLASSIFIED	UNCLASSIFIED	UNCLASSIFIED	UL	12	Brian Schuster
					19b. TELEPHONE NUMBER (*Include area code*) (410) 278-6020

A COMPARISON OF THE DEFORMATION, FLOW, AND FAILURE OF TWO TUNGSTEN HEAVY ALLOYS IN BALLISTIC IMPACTS

Brian Schuster and Lee Magness
Army Research Laboratory
Aberdeen Proving Ground
Aberdeen MD 21005-5066

ABSTRACT

Ballistic tests were conducted with sub-scale long rod penetrators of two different processing conditions of the same tungsten heavy alloy. The liquid-phase sintered composite of 90% tungsten-9% nickel –1% cobalt (by weight) was tested in its low-strength, as-sintered and heat-treated condition, and in a high-strength, 50% cold-worked (by swaging) and aged condition. Consistent differences in the ballistic performances of the two lots of penetrators were observed, in depth of penetration tests in thick armor steel targets and in limit velocity determinations against finite thickness steel targets. Metallographic examinations were conducted on the residual penetrators recovered from sectioned steel targets. Using the tungsten particles in the nickel alloy matrices of these residual penetrator materials as embedded strain gauges, the strain distributions, deformation gradients, and flow and failure behaviors of these two tungsten heavy alloy lots are examined.

INTRODUCTION

Differences, in the abilities of tungsten heavy alloys (WHA) of the same density to penetrate into heavy steel armor, are generally quite small and difficult to detect above the experimental errors associated with ballistic testing methods [Leonard and Magness (1)]. In recent quarter-scale ballistic tests, however, a consistent difference in ballistic performance, well outside experimental error, was observed for two different processing conditions of the same WHA. This prompted a more detailed series of tests, including recovery and examination of residual penetrators and comparisons of the deformation and failure behaviors of the two materials.

PROCESSING AND PROPERTIES OF THE TWO WHA LOTS

The two lots of WHAs were manufactured by GTE Sylvania, Inc. (now Osram-Sylvania, Inc.). Both lots were liquid-phase sintered tungsten (W) composites with compositions of 90% W – 9 % nickel – 1% cobalt (by weight), and identical densities of 17.25 g/cm^3. Both lots received a post-sinter heat treatment to re-solutionize a W_4Ni intermetallic compound [Myhre (2)]. Lot 1 was left in the as-sintered and heat-treated condition, while Lot 2 underwent additional cold-work of 50 % reduction-in-area (RA) by swaging, followed by an aging heat treatment (3 hours at 600°C). The quasi-static properties of the alloys are listed in Table I.

The quasi-static properties listed in Table I are close to the extreme limits possible for WHA through conventional processing techniques. The yield strength of the heavily worked Lot 2 is approximately 2 ½ times larger than the same material in the unworked condition. At larger strains, the differences are less dramatic (1000 vs. 1641 MPa ultimate strengths). At the very high strain rates occurring during ballistic impacts, the flow stresses of both alloys will be higher but their differences can be expected to be much smaller [Meyer et al (3), Coates and

Table I. Quasi-Static Properties of WHAs, Lot 1 and Lot 2

Material 90 W – 9 Ni – 1 Co	Rockwell C Hardness	Yield Strength (0.2%) (MPa)	Ultimate Strength (MPa)	Elongation to failure (%)	Unnotched Charpy Energy* (J)
Lot 1, As-Sintered & Heat-Treated	32	614	1000	34	89
Lot 2, Swaged 50% RA, Aged	49.9	1530	1641	7	12

* *Charpy values for 5 mm by 5mm bars*

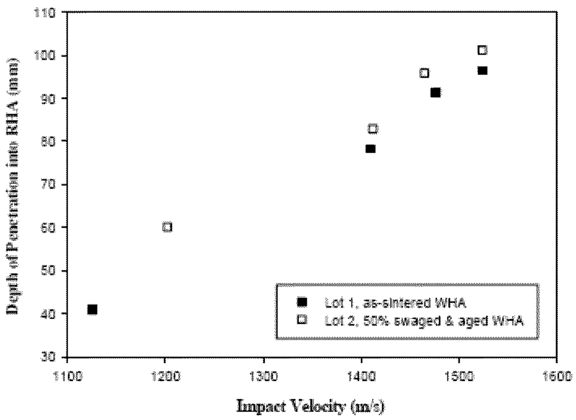

Figure 1. Depth of Penetration as a Function of Impact Velocity, Lot 1 and Lot 2 WHAs.

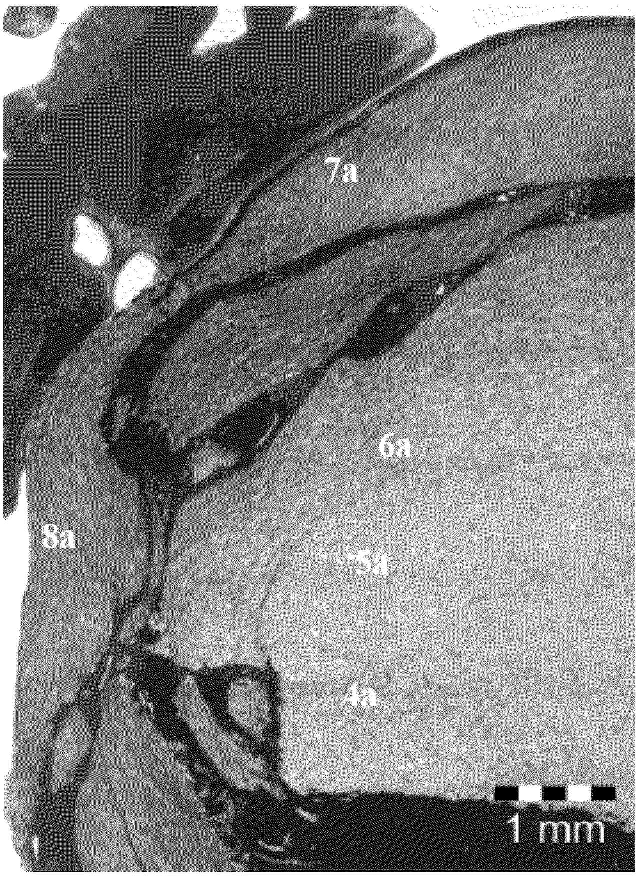

Figure 2: Shot #34. As-Sintered Penetrator Sectioned and polished. Etched with Murakami's reagant

Ramesh (4)]. In either case, the flow stress of the WHA penetrator material will be greatly exceeded by the shear stresses and hydrostatic pressures imposed on the head of the long rod penetrator.

BALLISTIC COMPARISON TESTS

For the ballistic testing, the WHA bar stock was machined into hemispherical-nosed, 65gram mass, long rod penetrators, with length-to-diameter (L/D) ratios of 15 or 20. The L/D = 20 rods have a diameter of 6.20mm and a length of 124.4mm. The L/D = 15 rods have a diameter of 6.83mm and a length of 102.4mm. A limit velocity, the velocity required to just perforate a given target, was determined for the penetrators of each alloy [Lambert and Jonas, (5)]. The target was a 76.2mm plate of Rolled Homogeneous Armor (RHA) at normal incidence [6]. The ballistic results are summarized in Table II.

For both alloys, the limit velocities decreased as the L/D ratio of the rods increased (and the longer penetrators brought the kinetic energy to bear upon a smaller presented area of the armor steel). At each L/D ratio, the higher strength Lot 2 alloy delivered a significantly lower limit velocity (by 30 to 40 m/s) than the as-sintered alloy.

Additional tests were conducted, firing L/D = 20 rods into 152mm thick RHA target blocks, over a range of impact velocities. The thick RHA targets were then sectioned to measure the penetration depths, and to recover the residual penetrators embedded in the steel for later metallographic examinations. The penetration test results are plotted in Figure 1. Consistent with the limit velocity results in Table II, the higher strength Lot 2 alloy achieved a greater depth of penetration at the same impact velocity than an as-sintered alloy.

METALLOGRAPHIC EXAMINATIONS OF RESIDUAL PENETRATORS

Overall views of the deformations of the as-sintered (Lot 1) and 50% swaged and aged (Lot 2) WHA penetrators are shown in Figures 2 and 3, respectively. The progression of the plastic deformation within each of the residual penetrators, at the selected points indicated in Figures 2 and 3, is illustrated by the micrographs

Table II. Limit Velocities for Lot 1 and Lot 2 WHAs against 76.2mm RHA Plate

Material	L/D = 15	L/D = 20
	Limit Velocity	Limit Velocity
90W – 9 Ni – 1 Co	(m/s)	(m/s)
Lot 1, As-Sintered & Heat-Treated	1380	1330
Lot 2, Swaged 50% RA, Aged	1340	1290

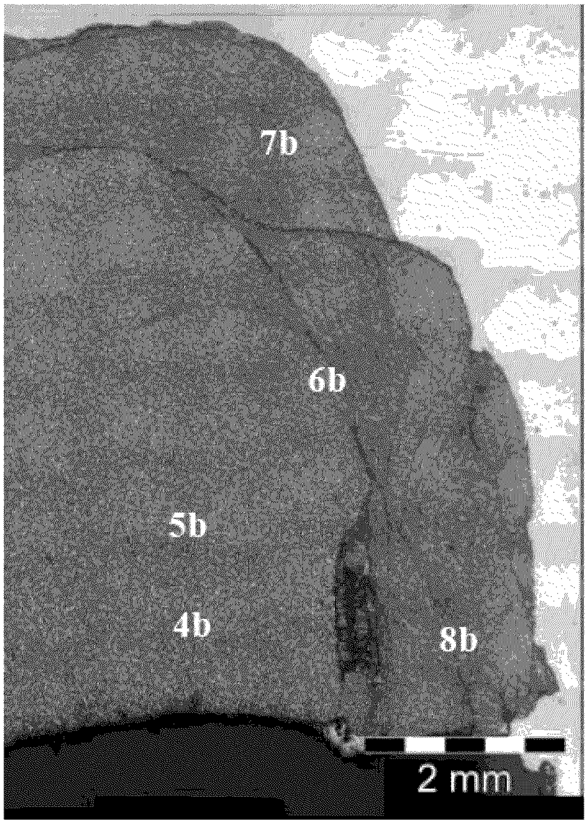

igure 3: Shot #33. Penetrator Swaged 50%. Sectioned and olished Etched with Murakami's reagant

of Figures 4-8a, and Figures 4-8b, respectively. The W particles embedded in the nickel alloy matrix serve as approximate strain gages; the aspect ratio (major to minor axis) of each W particle could be measured. The aspect ratios of a number of particles were measured and labeled in each of the micrographs. These results are summarized in Table III.

DISCUSSION

The contrast between the deformation and failure behaviors of the 90W-9Ni-1Co alloy in the two processing conditions is clearly illustrated by Figures 2 through 8. At the rear of the residual penetrators, the original WHA microstructures, with little or no deformation resulting from ballistic impact, can be compared. Nearly spherical (average aspect ratio of 1.24), randomly oriented W particles are found for the as-sintered (Lot 1) WHA in Figure 4a. Having undergone 50% RA by swaging, the corresponding microstructure for Lot 2 (Figure 4b) reveals an average aspect ratio of the W particles of approximately 2.49, oriented parallel to the original axis of the long rod penetrator. Both materials then undergo similar, but also distinctly different, progressions of deformation as the WHA rod lengths are fed into the mushroomed heads of the penetrators, are inverted, and then discarded along the walls of the penetration cavities.

Table III. Aspect Ratios and Statistics from Microstructural Figures

Figure	Min Aspect	Max Aspect	Mean	Std Dev	Sample Size
4A	1.0367	1.6036	1.2429	0.1297	20
4B	1.8094	3.4129	2.4902	0.4749	17
5A	1.5299	5.3273	2.8104	0.9321	26
5B	1.1777	2.1292	1.4873	0.2600	12
6A	2.3777	14.5603	7.2325	2.9835	23
6B	1.2905	3.9207	2.4608	0.7905	14
7A	3.1432	20.4137	8.6888	4.7214	17
7B	1.1209	6.3026	3.1380	1.3473	20
8A	4.3964	20.7785	11.4055	4.3474	18
8B	1.1265	3.4586	1.7867	0.5818	21

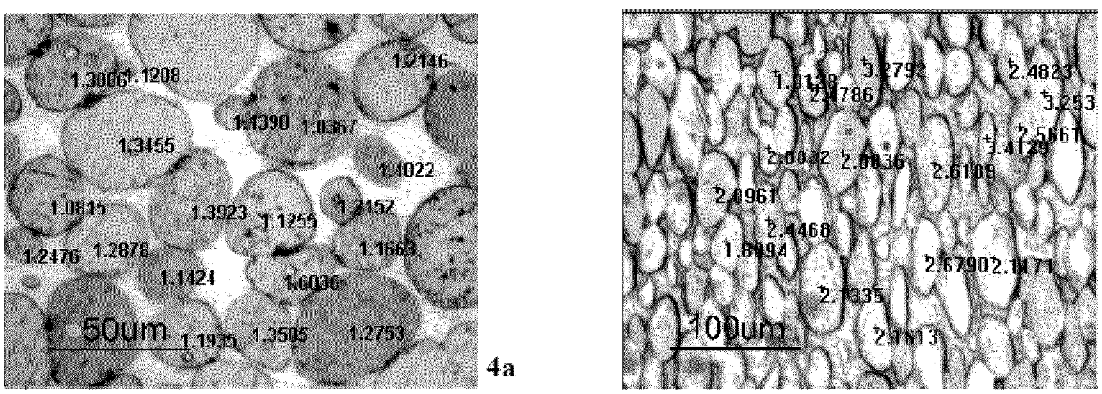

Figure 4: Undeformed microstructures near the back of the penetrators

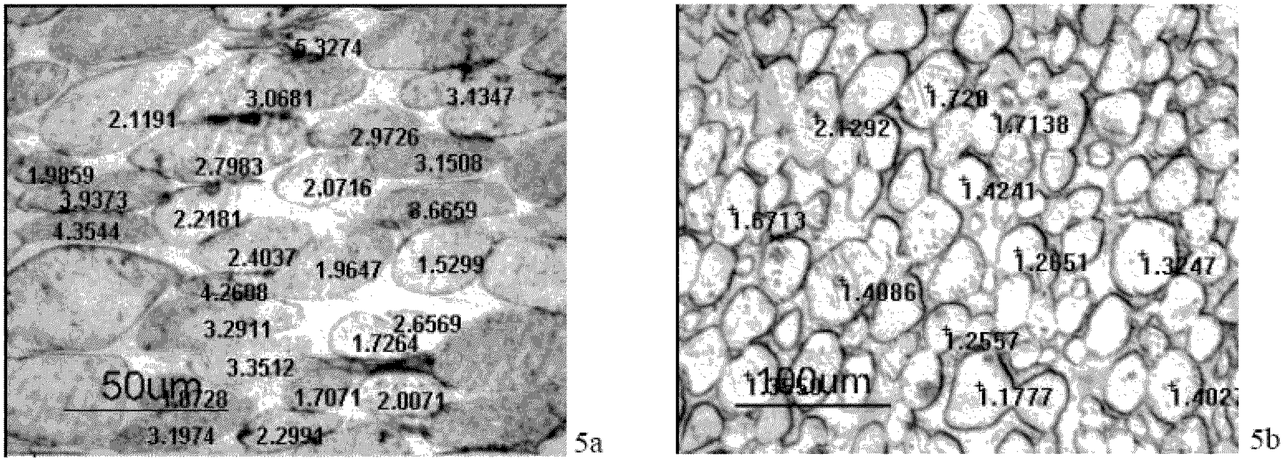

Figure 5. Moderately deformed microstructure in the mushroomed heads.

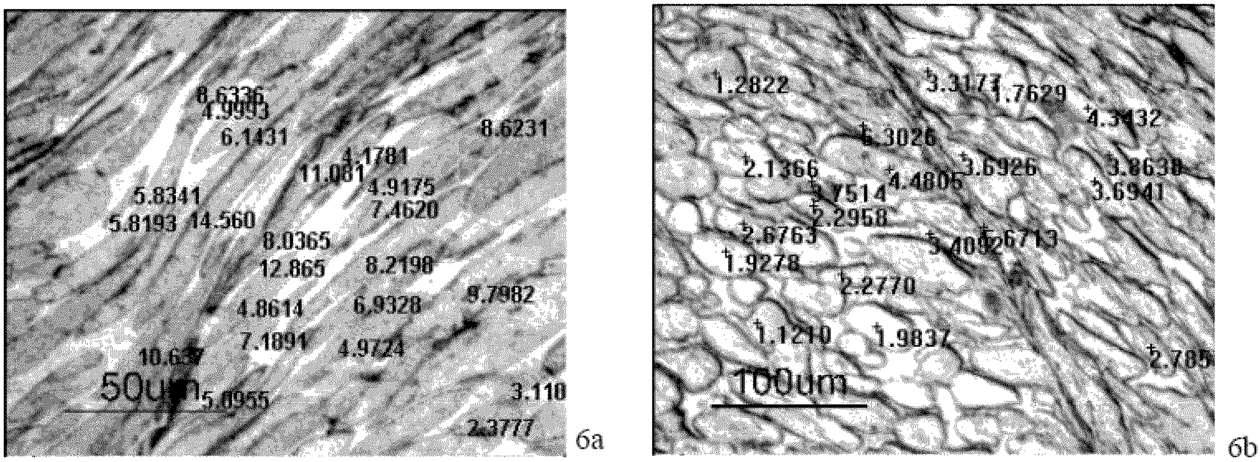

Figure 6. Strain localizations developing in the mushroomed heads.

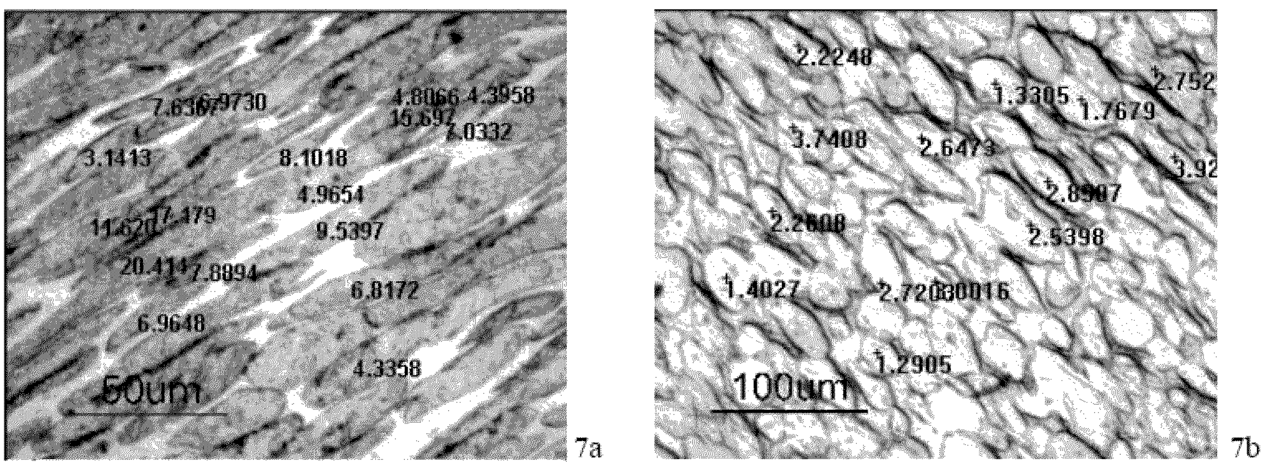

Figure7. Heavily deformed microstructures near penetrator-target interfaces at the head of the penetrators.

The nearly-spherical W particles in microstructure of the as-sintered WHA (Figure 4a) become flattened as the material approaches the penetrator-target interface (Figure 5a, average aspect ratio of 2.13). Plastic localizations develop at stress concentrations within the mushroomed head, amid W particles with aspect ratios of 5 or greater (Figure 6a). WHA material nearing the periphery of the mushroomed head (Figure 7a) and material discarded from the penetrator (Figure 8a), exhibit highly elongated W particles with aspect ratios of 8 and greater.

By contrast, the initially elongated W particles in the swaged Lot 2 WHA first recover their spherical shapes (Figure 5b, average aspect ratio decreasing to 1.48) be-

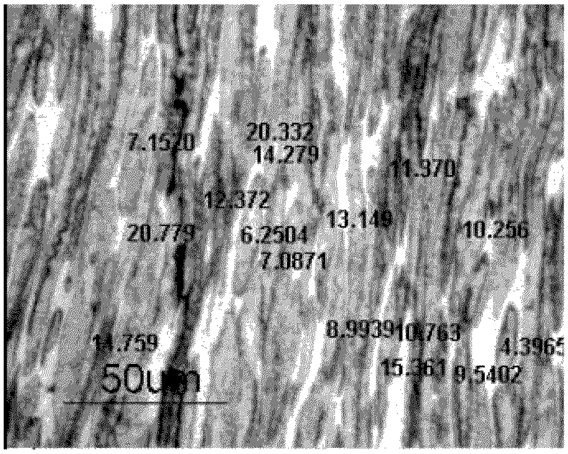

8a

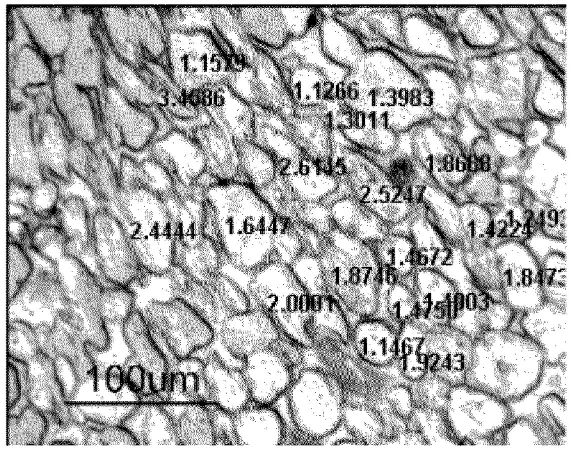

8a

Figure 8: Microstructures within the discarded chips of WHA

fore also beginning the process of flattening. Plastic localizations appear to develop more quickly (at lower accumulated strain levels) and more sharply in this material (Figure 6b). Highly elongated W particles do not develop in the WHA material nearing the periphery of the mushroomed head (Figure 7b, average aspect ratio of 3.14). Similarly, examinations of the fully eroded material (Figure 8b) reveal W particle aspect ratios of no more than 3.5 within the chips discarded by the penetrator.

A more rapid discard of deformed material from the heads of penetrators manufactured from the Lot 2 WHA would be consistent with their penetration and limit velocity performances being superior to those of the Lot 1 WHA. An analogous mechanism has been shown to be responsible for the superior performance of depleted uranium (DU) alloys over comparable density WHAs in penetrator applications [Magness and Farrand (7)]. The early failure and discard of the DU uranium penetrator material via adiabatic shear localization, prevents the build up of a large mushroomed head on these projectiles. DU penetrators thus can burrow narrower diameter, and therefore deeper, penetration cavities in armor. In comparable model-scale tests, DU penetrators defeat the 76.2mm target at limit velocities approximately 100 m/s lower than comparable WHA penetrators. Though not as dramatic, the 30 m/s improvement in the performance of the 90W-9Ni-1Co WHA with 50% cold-work, is the largest shift in limit velocities ever observed in these model scale tests.

CONCLUSIONS

Cold-work of 50% RA (by swaging), followed by an aging heat treatment, improved the penetration performance of a liquid-phase sintered 90W-9Ni-1Co composite into steel armor, Sub-scale, long rod penetrators of this heavily-worked alloy perforated a monolithic RHA steel target plate at velocities 30 to 40 m/s lower than for equivalent mass and geometry rods of the same alloy in the unworked condition. Metallographic examinations were conducted on the residual penetrators recovered from the ballistic tests. Significant differences were observed, in the distributions of the plastic deformation within the "mushroomed" heads that formed on the two sets of penetrators, in the number and the location of plastic localizations (shear bands) within the heads, and the level of microstructural deformation that occurred between the localizations. The deformation of the unworked lot of WHA penetrator material was more diffuse, i.e. more broadly distributed throughout the mushroomed head with less distinctive plastic localizations. The deformation of the worked lot of WHA penetrator material appears to focus more quickly into plastic localizations, resulting in less deformation within the chips of WHA discarded from the head of the penetrator. The differences in the flow and failure behaviors of these two lots of the 90W-9Ni-1Co alloy are consistent with the 30 to 40 m/s shift in their limit velocities.

REFERENCES

1. W. Leonard, L. Magness, and D. Kapoor, "Improving Mechanical Properties of Tungsten heavy Alloy Composites Through Thermomechanical Processing," Int. Conf. on Tungsten & Tungsten Alloys, MPIF, (1992), p.127.
2. T. Myhre, "Processing Description for Cold-Worked 90% Tungsten Alloy Rods," Union Carbide Corp.- Nuclear Div. Report Y/PG-2275 (1979).
3. L. Meyer, F. Behler, K. Frank, and L. Magness, "Interdependencies Between the Dynamic Mechanical Properties and the Ballistic Behavior of Materials," Proc. 12th Int. Symp. Ballistics (1990).
4. R. Coates and K.T. Ramesh, "The Rate-Dependent Deformation of a Tungsten Heavy Alloy," Mat Sc & Eng, A145 (1991), p.159.
5. J. Lambert and G. Jonas, "Towards Standardization in Terminal Ballistics Testing: Velocity Representation," U.S. Army Ballistic Research Laboratory Report, ARBRL-R-1852, (1976)
6. MIL-A-12560G(MR), Armor Plate, Steel, Wrought, Homogeneous (1984).
7. L. Magness and T. Farrand, "Deformation Behavior and Its Relationship to the Penetration Performance of High-Density KE Penetrator Materials," US Army Science Conf, (1990) 149.

NO. OF COPIES	ORGANIZATION
1 (PDF ONLY)	DEFENSE TECHNICAL INFORMATION CTR DTIC OCA 8725 JOHN J KINGMAN RD STE 0944 FORT BELVOIR VA 22060-6218
1	US ARMY RSRCH DEV & ENGRG CMD SYSTEMS OF SYSTEMS INTEGRATION AMSRD SS T 6000 6TH ST STE 100 FORT BELVOIR VA 22060-5608
1	INST FOR ADVNCD TCHNLGY THE UNIV OF TEXAS AT AUSTIN 3925 W BRAKER LN AUSTIN TX 78759-5316
1	DIRECTOR US ARMY RESEARCH LAB IMNE ALC IMS 2800 POWDER MILL RD ADELPHI MD 20783-1197
3	DIRECTOR US ARMY RESEARCH LAB AMSRD ARL CI OK TL 2800 POWDER MILL RD ADELPHI MD 20783-1197
3	DIRECTOR US ARMY RESEARCH LAB AMSRD ARL CS IS T 2800 POWDER MILL RD ADELPHI MD 20783-1197

ABERDEEN PROVING GROUND

NO. OF COPIES	ORGANIZATION
1	DIR USARL AMSRD ARL CI OK TP (BLDG 4600)

INTENTIONALLY LEFT BLANK.